Indian Journal of Pure & Applied Physics
Vol. 54, July 2016, pp. 431-438

Hydrostatic pressure and polaronic effects on the confined energies in a spherical quantum dot

A Rejo Jeice[a] & K S Joseph Wilson[b]*

[a]Department of Physics, Annai Velankannai College, Tholayavattam 629 157, India

[b]Departmant of Physics, Arul Anandar College, Madurai 625 514, India

Received 13 November 2013; revised 11 September 2014; accepted 9 January 2015

The confined energies of low lying 1*s*, 1*p* and 1*d* states of an electron in a spherical quantum dot have been found out with finite barrier. The effects of hydrostatic pressure on various barrier heights have also been found. The influence of polaronic effects has been analyzed. The results show that the confined energies decrease as the dot size increases, the effect of hydrostatic pressure and polaronic mass decrease the confined energy, and the combined effect of hydrostatic pressure and polaronic reduce the confinement to 12% and 22% for 1*s*, 1*p* and 1*d* states, respectively. The results are also in good agreement with the other research articles in the literature.

Keywords: Spherical quantum dot, Square well confinement, Confined energies, Effective mass approximation

1 Introduction

In the last few decades, the properties of low-dimensional semiconductor systems (LDSS)[1,2] have attracted much attention in theoretical and applied physics. The study of various LDSS becomes important in quantum mechanics due to the quantum confinement[3]. The recent development and advances in nano fabrication technology such as molecular beam epitaxy (MBE)[4] and metal organic chemical vapor deposition (MOCVD)[5] or self-assembled method have made possible to manufacture different sizes and shapes of semiconductor quantum dots (QD's)[6,7], quantum wires[8] and quantum well[9] with their applications extend over many areas. In the quasi-zero-dimensional system (QD) since the carrier motion is restricted to a narrow region of a few nanometers in dimension and hence the study of confinement is interesting.

The effects of hydrostatic pressure on QD were studied by many of the researchers[10-18]. John Peter[10] has calculated the ionization energies in external perturbations such as hydrostatic pressure and magnetic field with a parabolic confinement for finite barrier quantum dots. He found that the ionization energy is purely pressure dependent and for smaller dot sizes the hydrostatic pressure dominates. Gerardin Jayam *et al.*[11] studied the effects of a static electric field and hydrostatic pressure on the donor binding energies for a spherical QD with parabolic confinement. They found that the ionization energy increases with hydrostatic pressure. Perez-Merchancano *et al.*[12] found that the donor and acceptor binding energies increase with the hydrostatic pressure for any position of the impurity in a spherical QD. Barseghyan *et al.*[13] found that in the low pressure regime the impurity binding energy growths linearly with pressure and in the high pressure regime the binding energy growths up to a maximum and then decreases in a QD. Xia *et al.*[14] investigated the hydrostatic pressure effects on the donor binding energy of a hydrogenic impurity in InAs/GaAs self-assembled quantum dot. Karimi *et al.*[15] studied the linear and nonlinear optical properties of multilayered spherical quantum dots under hydrostatic pressure. Rezaei *et al.*[16] have calculated the effects of the electric field, hydrostatic pressure and temperature on the binding energy in spherical QD. Sivakami *et al.*[17] had studied the effects of hydrostatic pressure and conduction band non-parabolicity on the impurity binding energy in a spherical QD. The effects of hydrostatic pressure and polaronic mass on the correlation energies have been studied in a spherical QD[18]. In the present manuscript, the hydrostatic pressure and polaronic effects have been analyzed in the spherical quantum dot on the confined energy varying the barrier height.

*Corresponding author (E-mail: wilsonpra@yahoo.co.in)

The purpose of the present work is to extend the calculation of our previous work[18] by varying the aluminum concentration (x = 0.1–0.4) to 1s, 1p and 1d states of an electron in a spherical QD. In the present work, we have considered a GaAs QD embedded in a $Ga_{1-x}Al_xAs$ matrix with finite barriers. The barrier height depends on x. When an electron is introduced into the dot, the total energy of the system, by assuming it as spherical dot potential is estimated for different barrier heights.

2 Models and Calculations

2.1 Single electron in a spherical quantum dot

We consider a single electron in a spherical quantum dot in the finite barrier model. In the absence of impurity, within the effective mass approximation, the Hamiltonian is given by:

$$H_1 = -\frac{\hbar^2}{2m^*(P)}\nabla^2 + V_D(r,P) \qquad \ldots (1)$$

where $m^*(P)$ is the effective mass of the electron at the conduction band minimum, which is $0.067m_0$ for GaAs[19], where m_0 is the free electron mass. In our numerical calculations we use atomic units in which $m_0 = e^2 = \hbar^2 = 1$. The confining potential $V_D(r, P)$ is given by:

$$V_D(r,P)\begin{cases} 0 & r \le R \\ V_0 = Q_c \Delta E_g(x,P) & r \ge R \end{cases} \qquad \ldots (2)$$

where V_0 is the barrier height, Q_c is the conduction band offset parameter which is taken to be 0.6[20]. The band gap difference depends of the concentration of Al. In our case $Ga_{1-x}Al_xAs$ is the barrier medium in which GaAs dot is embedded. The total energy difference between the dot and barrier media, as a function of x, is given by[11]:

$$\Delta E_g(x) = 1.155x + 0.37x^2 \qquad \ldots (3)$$

In the present work we have chosen x = 0.1, 0.2, 0.3 and 0.4, and the values of V_0 turns to be 71.21, 147.48, 227.88 and 312.72 meV, respectively. Three lowest lying bound states are given by:

$$\psi_{1s}(\vec{r}) = \begin{cases} N_1 \dfrac{\sin(\alpha_1 r)}{\alpha_1 r} & r \le R \\ A_1 \dfrac{e^{-\beta_1 r}}{\beta_1 r} & r \ge R \end{cases} \qquad \ldots (4)$$

$$\psi_{1p}(\vec{r}) = \begin{cases} N_2\left[\dfrac{\sin(\alpha_2 r)}{(\alpha_2 r)^2} - \dfrac{\cos(\alpha_2 r)}{(\alpha_2 r)}\right]\cos\theta & r \le R \\ iA_2\left[\dfrac{1}{\beta_2 r} + \dfrac{1}{(\beta_2 r)^2}\right]e^{-\beta_2 r}\cos\theta & r \ge R \end{cases} \qquad \ldots (5)$$

$$\psi_{1d}(\vec{r}) = \begin{cases} N_3\left[\left(\dfrac{3}{(\alpha_3 r)^3} - \dfrac{1}{\alpha_3 r}\right)\sin(\alpha_3 r) - \dfrac{3}{(\alpha_3 r)^2}\cos(\alpha_3 r)\right](3\cos^2\theta - 1) & r \le R \\ A_3\left[\dfrac{1}{\beta_3 r} + \dfrac{1}{(\beta_3 r)^2} + \dfrac{1}{(\beta_3 r)^3}\right]e^{-\beta_3 r}(\cos^2\theta - 1) & r \ge R \end{cases} \qquad \ldots (6)$$

where N_1, N_2, N_3, A_1, A_2 and A_3 are normalization constants and α_1 and β_1 are given by:

$$\alpha_i = \sqrt{2m^*(P)E(P)} \text{ and } \beta_i = \sqrt{2m^*(P)(V_0 - E)(P)}$$

Matching the wave function and their derivatives at the boundary $r = R$, we get:

$$A_1 = N_1 \sin(\alpha_1 R)e^{\beta_1 R} \qquad \ldots (7)$$

$$A_2 = -iN_2\left(\frac{\beta_2}{\alpha_2}\right)^2\left(\frac{\sin(\alpha_2 R) - \alpha_2 R\cos(\alpha_2 R)}{\beta_2 R + 1}\right)e^{\beta_2 R} \qquad \ldots (8)$$

$$A_3 = N_3\left(\frac{\beta_2}{\alpha_2}\right)^2\left(\frac{(3 - (\alpha_3 R)^2)\sin(\alpha_3 R) - 3\alpha_3 R\cos(\alpha_3 R)}{(\alpha_3 R)^2 + 3\beta_3 R + 3}\right)e^{\beta_3 R} \qquad \ldots (9)$$

The energy eigen values are determined by imposing the Ben Daniel and Duke boundary condition[21]:

$$-\frac{i\hbar}{m_1^*(P)}\frac{\partial\psi}{\partial r}(r \le R)\bigg|_{r=R} = -\frac{i\hbar}{m_2^*(P)}\frac{\partial\psi}{\partial r}(r \ge R)\bigg|_{r=R}$$

We obtain:

$$\alpha_1 R + \beta_1 R\tan(\alpha_1 R) = 0 \quad \text{for } s\text{-states} \qquad \ldots (6)$$

$$\frac{\cot(\alpha_2 R)}{\alpha_2 R} - \frac{1}{(\alpha_2 R)^2} = \frac{1}{\beta_2 R} + \frac{1}{(\beta_2 R)^2} \quad \text{for } p\text{-states and} \qquad \ldots (11)$$

$$(9\alpha_3 R - (\alpha_3 R)^3) + (4(\alpha_3 R)^2 - 9)\tan(\alpha_3 R) = -[(3 - (\alpha_3 R)^2\tan(\alpha_3 R) - 3(\alpha_3 R)]$$

$$x\left(\frac{(\beta_3 R)^3+4(\beta_3 R)^2+9(\beta_3 R)+9}{(\beta_3 R)^2+3\beta_3 R+3}\right) \qquad \text{for } d\text{-states} \quad \ldots (12)$$

If $m_1^*(P) = m_2^*(P) = m^*(P)$, solving these transcendental equations numerically, the confined energies E_l^n (n = 1, 2, 3…; l=0,1,3) are obtained. For other excited states similar equations may be obtained when l = 3, 4… The confined energy for the first three states for various barrier heights is given in Tables 2-5.

2.2 Effect of Polaronic mass

The conduction band of GaAs is known to have non-parabolicity and a correction to the effective mass pertinent to the conduction band minimum is given[22] by:

$$m_{np}^*(P) = 0.067\left(1+\frac{\Gamma_E}{0.067}\right) \quad \ldots (13)$$

where $\Gamma_E = 0.0436 + 0.236E^2 - 0.147E^3$ in which E is the sub-band energy expressed in eV. GaAs is a polar semiconductor and piezoelectric, the electron interacts with the polar optical modes and acoustic modes via the Frőhilch coupling. Here additional enhancement of the effective mass is expected. This is referred to as the polaronic mass which may be obtained from:

$$\frac{1}{m_p^*(P)} = \frac{1}{m_{np}^*(P)}\left(1-\frac{\alpha_{eff}}{6}\right) \quad \ldots (14)$$

where α_{eff} is Frohlich coupling constant which is taken as 0.26[23].

2.3 Effect of hydrostatic pressure

Studies on the confined energy under external perturbations such as hydrostatic pressure with the polaronic effect are sparse. However, it is interesting to see to what extent the confined energies are affected by the hydrostatic pressure. Due to the application of hydrostatic pressure, the lattice constants, effective mass, barrier height and dot size are modified[11,24]. Hence we write all the expressions for these quantities as a function of hydrostatic pressure. The variation of dot size with pressure is given[11] by:

$$R(P)=R_0(1-1.5082\times 10^{-3}P) \quad \ldots (15)$$

where R_0 is the zero pressure quantum dot radius. It is known that $da/dP = -2.6694\times10^{-4}a_0$, where a_0 is the lattice constant of GaAs[25].The effective mass of the electron in the dot changes[11] as:

$$m(P)=m^*(0)e^{0.078P} \quad \ldots (16)$$

where P is expressed in GPa (1 kbar = 0.1 GPa). We assume that the band gap discontinuity in a GaAs-$Ga_{1-x}Al_xAs$ quantum dot heterostructures is distributed to about 40% on the valance band and 60% on the conduction band, with the total band gap difference between GaAs dot and $Ga_{1-x}Al_xAs$ barrier and it is given[18] as:

$$\Delta E(x, P) = \Delta E_g(x)+PD(x) \quad \ldots (17)$$

$\Delta E_g(x)$ is given in Eq. (3) and $D(x)$ is the pressure co-efficient on the band gap is given in:

$$D(x) = -[1.3\times 10^{-2}]x \quad \ldots (18)$$

The height of the potential barrier is measured as a function of Al concentration x and the hydrostatic pressure is given by[20]:

$$V(x) = 0.60x\,\Delta E(x, P) \quad \ldots (19)$$

Using these expressions, the confined energies for 1s, 1p and 1d states are calculated. In our calculation the pressure used was 4 GPa, which corresponds to 40 kbar. We have not considered the pressures beyond 4 GPa, because there is a direct to indirect band gap transition of GaAs occurs at about 4 GPa[18].

3. Results and Discussion

The results obtained are shown in Tables 1-5 and Figs 1-5. We have computed the combined effect of hydrostatic pressure and polaronic effects on the spherical quantum dot. Due to the application of the hydrostatic pressure on the spherical quantum dot the lattice constant, effective mass, barrier height and dot radius are modified. For varies hydrostatic pressure the variation of effective mass, dot radius and barrier height are given in Table 1. In addition, the variation of polaronic mass is also given Table 1. We have noticed that due to the application of hydrostatics pressure the dot size and barrier height are decreases and the effective mass increases. The variation of confined energies with dot radius for the barrier concentration x = 0.1, 0.2, 0.3 and 0.4 for E_{1s}, E_{1p} and E_{1d} states are given in Tables 2-5. In each case we found that the confined energy decreases as the dot radius increases for all the states as expected, as feature that is well known literatures[26-28]. The above results are also well agreement with Cantele *et al.*[29]

Table 1–Variation of the effective mass, barrier height and dot size of GaAs with pressure (x is corresponding to aluminum concentration of $Ga_{1-x}Al_xAs$)

Pressure (GPa)	$m_p(P)$ (a. u.)	$V_O(P)$ (meV)			$R(P)$ (Å)		
		x=0.2	x=0.3	x=0.4	x=0.2	x=0.3	x=0.4
0	0.067 (0.077)	147.48	227.88	312.72	50	150	300
1	0.072 (0.083)	147.324	227.646	312.408	49.925	149.774	299.548
2	0.078 (0.090)	147.168	227.412	312.096	49.849	149.548	299.095
3	0.085 (0.097)	147.012	227.178	312.784	49.774	149.321	298.643
4	0.092 (0.106)	146.856	226.944	311.472	49.698	149.095	298.19

Numbers within the brackets refer to the effective mass in the absence of polaronic mass effect

Table 2 – Confined energies under hydrostatic pressure in the finite barrier model for E_{1s} state (x=0.1 and 0.2). Dashes represent the unbound states

Dot radius (Å)	Confined energy (meV)					
	x=0.1			x=0.2		
	P=0 GPa	P=2 GPa	P=4 GPa	P=0 GPa	P=2 GPa	P=4 GPa
35	-	-	-	137.07 (142.74)	129.35 (136.57)	120.31 (128.32
40	-	-	-	122.93 (130.69)	119.03 (122.39)	104.33 (112.86)
50	66.71 (69.39)	63.00 (66.46)	58.64 (62.49)	96.19 (104.53)	87.34 (95.71)	78.61 (86.43)
100	29.61 (32.78)	26.42 (29.44)	23.38 (26.09)	34.50 (38.66)	30.44 (34.29)	26.63 (30.02)
150	15.56 (17.45)	13.72 (15.47)	11.98 (13.52)	17.20 (19.44)	15.05 (17.10)	13.07 (14.84)
200	9.50 (10.74)	8.33 (9.45)	7.24 (8.21)	10.25 (11.64)	8.93 (10.19)	7.72 (8.80)
250	6.39 (7.24)	5.59 (6.35)	4.84 (5.50)	6.79 (7.73)	5.91 (6.75)	5.10 (5.81)
300	4.59 (5.21)	4.00 (4.57)	3.46 (3.93)	4.82 (5.50)	4.19 (4.80)	3.61 (4.12)

Numbers within the brackets refer to the confined energies in the absence of polaronic mass effect

for a single electron to the ellipsoidal QD. We also notice that it is higher in the absence of polaronic mass and decreases when the pressure increases for all dot size. This behavior is due to variation of mass with the change in pressure.

In Table 2 we observe that there are no bound 1*s* states for dot size less than 50 Å and 35 Å since the barrier height itself 71.21 meV and 147.48 meV, respectively. The physical origin of the above result is that we had considered the finite barrier spherical quantum dot. We cannot found the barrier height for dot radii less than 50 Å and 35 Å, respectively. Similarly in Table 3 we observe that there is no bound 1*s* state for dot size less than 30Å since the barrier height itself 227.88 meV and 312.72 meV, respectively. Similar observations were found in Tables 4-5 for E_{1p} and E_{1d} states. The above observations are contrast to the quantum well case (Q2D system) where for every well size and barrier height a bound state is always assured[30]. Another observation is that the *p*-state energies are approximately two times the corresponding *s*-state energies. Thus we conclude that the energy is higher in smaller dot radii of higher barrier concentration (x=0.4). Thus, the concentration of aluminum is more important in conduction band of $Ga_{1-x}Al_xAs$[19].

Figure 1 shows the variation of confined energy as a function of dot size for the E_{1s} state with barrier

Table 3–Confined energies under hydrostatic pressure in the finite barrier model for E_{1s} state (x=0.3 and 0.4)

Dot radius (Å)	Confined energy (meV)					
	x=0.3			x=0.4		
	P=0 GPa	P=2 GPa	P=4 GPa	P=0 GPa	P=2 GPa	P=4 GPa
30	202.02	188.87	174.27	238.46	219.02	198.96
	(212.67)	(201.21)	(187.24)	(256.07)	(237.36)	(216.82)
35	173.53	160.36	145.71	199.17	180.71	162.35
	(187.34)	(173.73)	(158.75)	(216.74)	(198.17)	(178.71)
40	149.65	136.01	122.39	167.14	150.45	134.15
	(162.55)	(148.89)	(134.52)	(183.47)	(166.25)	(148.67)
50	111.28	99.83	88.74	121.08	107.88	95.30
	(122.56)	(110.67)	(98.60)	(134.32)	(120.38)	(106.50)
100	36.90	32.40	28.22	38.43	33.64	29.23
	(41.57)	(36.67)	(31.59)	(43.43)	(38.20)	(33.16)
150	17.99	15.70	13.59	18.50	16.10	13.90
	(20.40)	(17.89)	(15.46)	(21.02)	(18.38)	(15.86)
200	10.60	9.22	7.95	10.83	9.40	8.10
	(12.07)	(10.54)	(9.08)	(12.34)	(10.75)	(9.26)
250	6.99	6.06	5.22	7.09	6.16	5.29
	(7.95)	(6.94)	(5.97)	(8.10)	(7.05)	(6.06)
300	4.94	4.29	3.69	5.02	4.34	3.72
	(5.63)	(4.90)	(4.22)	(5.72)	(4.97)	(4.28)

Numbers within the brackets refer to the confined energies in the absence of polaronic mass effect

Table 4 – Confined energies under hydrostatic pressure in the finite barrier model for E_{1p} state (dashes represent the unbound states)

Dot radius (Å)	Confined energy (meV)							
	x=0.1		x=0.2		x=0.3		x=0.4	
	P=0 GPa	P=4 GPa	P=0 GPa	P=4 GPa	P=0 GPa	P=4 GPa	P=0 GPa	P=4 GPa
50							238.10	190.38
	-	-	-	-	-	-	(261.17)	(211.48)
65	-	-	130.82	104.12	149.55	118.11	161.01	125.47
			(140.75)	109.26	(165.3)	(131.87)	(179.56)	(140.93)
100	57.81	46.53	70.21	54.00	74.95	57.45	77.27	59.61
	(63.15)	(51.55)	(77.73)	(60.74)	(84.29)	(64.99)	(88.35)	(67.61)
150	31.45	24.32	35.40	26.65	36.74	27.75	37.78	28.42
	(35.17)	(27.41)	(39.57)	(30.26)	(41.64)	(31.59)	(42.90)	(32.42)
200	19.35	14.75	21.16	15.78	21.67	16.26	22.14	16.55
	(21.81)	(16.73)	(23.75)	(17.98)	(24.65)	(18.56)	(25.22)	(18.94)
250	13.04	9.88	14.00	10.41	14.27	10.67	14.52	10.83
	(14.76)	(11.22)	(15.80)	(11.89)	(16.27)	(12.20)	(16.56)	(12.40)
300	9.34	7.06	9.99	7.39	10.10	7.54	10.24	7.43
	(10.64)	(8.04)	(11.25)	(8.44)	(11.54)	(8.62)	(11.70)	(8.74)

Numbers within the brackets refers to the confined energies in the absence of polaronic mass effect

concentration x=0.1. We observe that the confined energy reduces to 4% for lower dot radii in the presence of polaronic effect and is negligible for larger dot size.

Figure 2 shows the variation of confined energy as a function of dot size for the E_{1s} state with barrier concentration when x=0.2 and 0.4, respectively. We also observe due to the application of hydrostatic pressure and polaronic mass to the lower dot radii confined energy reduces to 12% when x=0.2 and 17% when x=0.4. Hence we conclude that for E_{1s} state the hydrostatic pressure increases the percentage of reduction in confined energy. The above result is in agreement with the results of Bednarek *et al.*[31] were the quantum well system with parabolic confinement is considered.

Figure 3 shows the variation of confined energy as a function of dot size for the E_{1p} state with barrier concen ıtion when x=0.1 and 0.3, respectively. There are no bound state for do t radii smaller than 65Å

Table 5 – Confined energies (meV) under hydrostatic pressure in the finite barrier model for E_{1d} state (dashes represent the unbound states)

Dot radius (Å)	Confined energy (meV)							
	x=0.1		x=0.2		x=0.3		x=0.4	
	P=0 GPa	P=4 GPa	P=0 GPa	P=4 GPa	P=0 GPa	P=4 GPa	P=0 GPa	P=4 GPa
65	-	-	-	-	-	-	258.54 (285.72)	203.57 (227.70)
75	-	-	-	-	192.65 (212.58)	151.98 (169.86)	207.25 (231.27)	160.87 (181.00)
100	-	-	112.23 (124.58)	87.81 (98.47)	122.2 (137.09)	94.00 (106.16)	128.07 (144.36)	97.72 (110.75)
150	50.86 (56.62)	39.63 (44.52)	57.37 (64.71)	43.72 (49.57)	60.28 (68.29)	45.58 (51.86)	65.05 (70.46)	46.71 (53.26)
200	31.63 (35.61)	24.19 (27.39)	34.37 (38.98)	25.93 (29.54)	35.63 (40.51)	26.73 (30.52)	36.39 (41.46)	27.23 (31.13)
250	21.4 (24.21)	16.21 (18.43)	22.82 (25.95)	17.12 (19.55)	23.47 (26.76)	17.54 (20.06)	23.88 (27.25)	17.8 (20.38)
300	15.40 (17.46)	11.60 (13.22)	16.24 (18.50)	12.14 (13.88)	16.62 (18.97)	12.39 (14.18)	16.86 (19.26)	12.54 (14.37)

Numbers within the brackets refers to the confined energies in the absence of polaronic mass effect

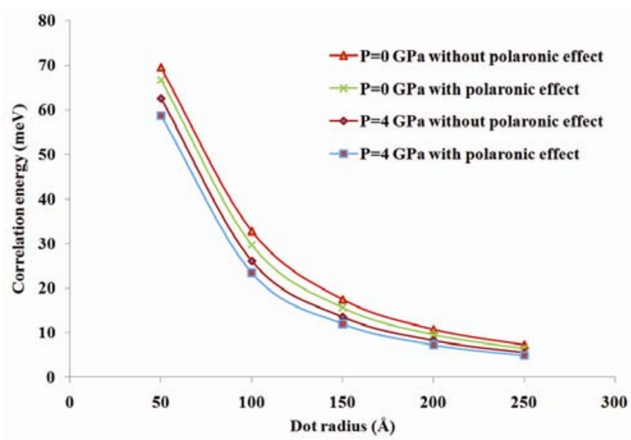

Fig. 1 – Variation of confined energy vs dot radius in the finite barrier model for E_{1s} state when x = 0.1

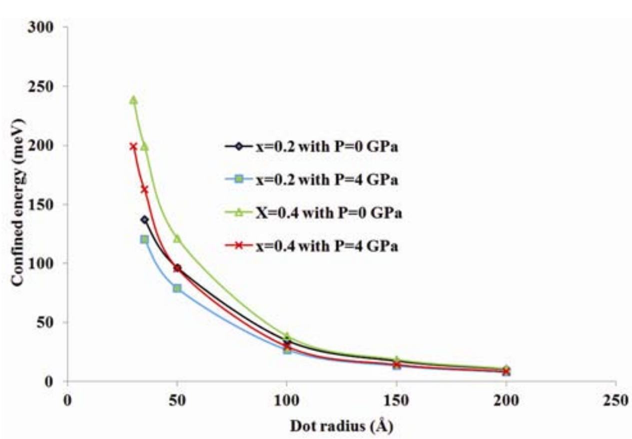

Fig. 2 – Variation of confined energy vs dot radius in the finite barrier model for E_{1s} state when x=0.2 and 0.4

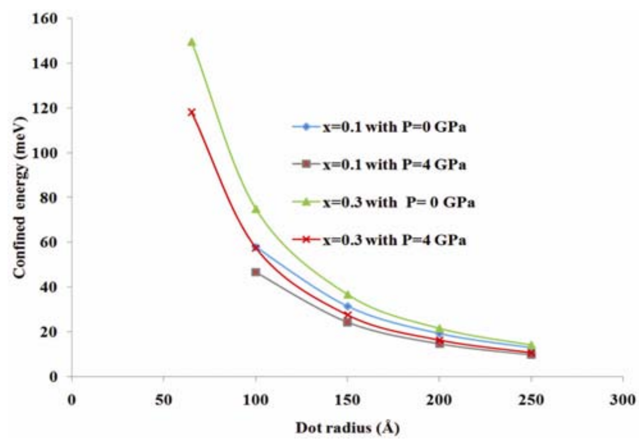

Fig. 3 – Variation of confined energy vs dot radius in the finite barrier model for E_{1p} state when x=0.1 and 0.3

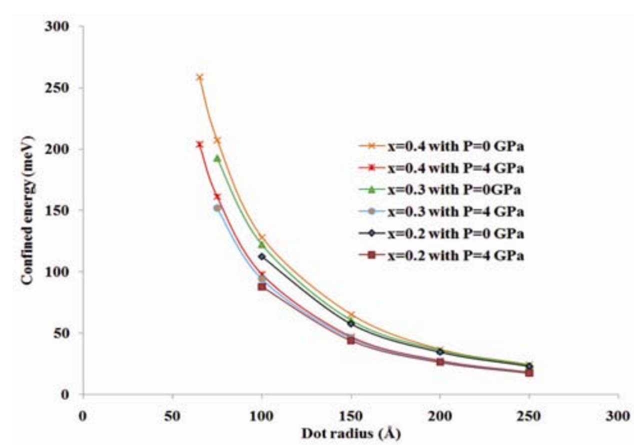

Fig. 4 – Variation of confined energy vs dot radius in the finite barrier model for E_{1d} state when x=0.2, 0.3 and 0.4

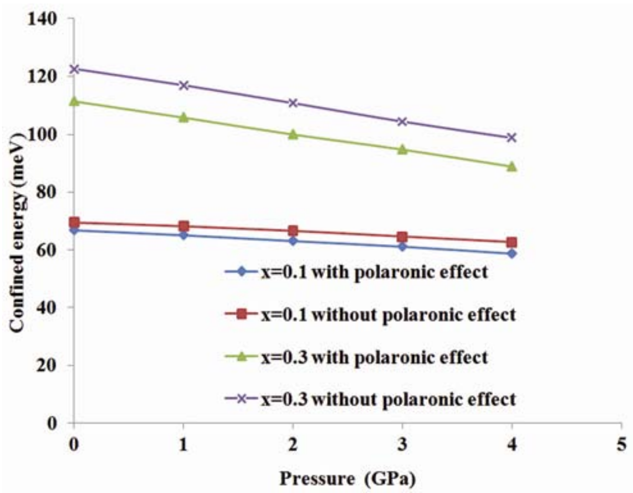

Fig. 5 – Variation of confined energy vs pressure in the finite barrier model for dot radius 50 Å (*1s* -state)

when x=0.1 and 100 Å when x=0.3, respectively. Also for lower dot radius the confined energy reduces to 20% when x=0.1 and 21% when x=0.3.

Figure 4 shows the variation of confined energy as a function of dot size for the E_{1d} state with barrier concentration when x=0.2, 0.3 and 0.4, respectively. There are no bound state for dot radii smaller than 100Å, 75 Å and 65Å when x=0.1 0.3 and 0.4, respectively. For the 1d state the confined energy reduces to 20-22% for lower dot radii.

Thus the confinement in narrow dot system operating under hydrostatic pressure and polaronic mass may be used to tune the output of the optoelectronic devices without modifying the physical size of quantum dot.

Figure 5 shows the variation of confined energy with pressure for dot size of 50 Å for the E_{1s} state barrier concentration 0.1 and 0.3, respectively. It has been seen that the pressure increases the confined energy decreases linearly. The important conclusion that emerges from the result of Tables 2-5 and Figs. 1-4 is that the hydrostatic pressure and polaronic effect are important for smaller dots and should be considered in the studies of LDSS. Thus the effect of hydrostatic pressure reduces the confinement to 9-19% and polaronic mass to 4-10%. Thus the combined effect of hydrostatic pressure and polaronic mass reduces the confinement to 12-22% for 1s and 1p states, respectively.

4 Conclusions

We investigated the effects of hydrostatic pressure and polaronic mass on the confined energies in a spherical quantum dot. It was found that the confined energy decreases due to the application of hydrostatic pressure and the variation are higher in smaller dot of higher aluminum concentrations. It approaches to zero as the dot radius approaches to infinity for all the states. The conduction band non-parabolicity and the polaronic effect have reduced the further energy.

Acknowledgment

The authors would like to thank Prof. K Navaneethakrishnan, School of Physics, Madurai Kamaraj University for his encouragement and valuable suggestion.

References

1 Delerue C & Lannoo M, *Nanostructures: Theory and modeling,* (Springer, Berlin), 2004.
2 Harrison P, in *Theoretical and computational physics of semiconductor nanostructures*, 3rd ed, Wiley, 2010.
3 Dzyubenko A B & Yablonskii A L, *Phys Rev B*, 53 (1996) 16355.
4 Milanovic V & Ikonic Z, *Phys Rev B*, 39 (1989) 7982.
5 Parascandolo G, *Phys Rev B*, 68 (2003) 245318.
6 Bednarek S, Szafran B & Adamowski J, *Phys Rev B*, 59 (1999) 13036.
7 Erdogan I, Akankan O & Akbas H, *Physica E*, 33 (2006) 83.
8 Gammon, D, *Nature*, 405 (2000) 899.
9 Szafran B, Adamowski J & Bednarek S, *Physica E*, 5 (2000) 185.
10 John P A, *Solid State Commun*, 147 (2008) 296.
11 Gerardin Jeyam Sr & Navaneethakrishnan K, *Solid State Commun*, 126 (2003) 681.
12 Perez-Merchancano S T, Franco R & Silva-Valencia J, *Microelectron J*, 39 (2008) 383.
13 Barseghyan M G, Kirakosyan A A & Duque C A, *Eur Phys J*, 72 (2009) 521.
14 Xia C, Liu Y & Wei S, *Appl Surf Sci*, 254 (2008) 3479.
15 Karimi M J, Rezaei G & Nazari M, *J Lum,* 145 (2014) 55.
16 Rezaei G & Kish S S, *Physica E*, 45 (2012) 56.
17 Sivakami A & Mahendran M, *Physica B*, 405 (2010) 1403.
18 Sivakami A, Rejo J A & Navaneethakrishnan K, *Int J Mod Phys B*, 24 (2010) 5561.
19 Madelung O Ed, *Semiconductor basic data*, 2nd ed, (Springer-Verlag), 1996.
20 Daries Bella R S & Navaneethakrishnan K, *Solid State Commun*, 130 (2004) 773.
21 Li Y, Voskoboynikov O, Liu J L, Lee C P & Sze S M, *Nanotechnology*, 1 (2001) 562.
22 Chaudhuri S & Bajaj K K, *Phys Rev B*, 29 (1984) 1803.
23 Benedictal A, Sukumar B & Navaneethakrishanan K, *Phys State Solid B*, 178 (1993) 167.
24 Moscoso-Moreno C A, Franco R & Silva-Valencia J, *Rev Mex Fis*, 53 (2007) 189.

25 Adachi S, GaAs & related materials, 1st ed, (World Scientific, Singapore), 1994.
26 Rejo Jeice A & Navaneethakrishnan K, *Braz J Phys*, 39 (2009) 526.
27 Sivakami A & Navaneethakrishnan K, *Physica E*, 40 (2008) 649.
28 Sadeghi E & Hosseini F, *J Basic Appl Phys*, 1 (2012) 66.
29 Cantele G, Ninno D & Iadonsi G, *Phys Rev B*, 64 (2001) 125325.
30 Mitin V V, Kochelap V A & Stroscio M A, *Micro electronics and optoelectronics*, (Cambridge University Press, Cambridge), 1999.
31 Bednarek S, Chwiej T, Adamowski J & Szafran B, *Phys Rev B*, 61 (2003) 205316.